Quasi In Situ XPS on a SiO x F y Layer Deposited on Silicon by a Cryogenic Process

G. Antoun, A. Girard, T. Tillocher, P. Lefaucheux, J. Faguet, K. Maekawa, C. Cardinaud, R. Dussart

Quasi *in situ* XPS on a SiO_xF_y layer deposited on Silicon by a cryogenic process

G. Antoun[1], A. Girard[2], T. Tillocher[1], P. Lefaucheux[1], J. Faguet[3], K. Maekawa[4], C. Cardinaud[2z], R. Dussart[1z]

[1]GREMI, Université d'Orléans, CNRS, 14 Rue d'Issoudun BP 6744, 45067 Orléans, France
[2]IMN, Institut des Matériaux Jean Rouxel, Université de Nantes, CNRS, BP32229, 44322 Nantes Cedex 3, France
[3]Tokyo Electron America, Inc., 2400 Grove Blvd., Austin, Texas 78741, USA
[4]TEL Technology Center, America, LLC, NanoFab 300 South 255 Fuller Rd., Suite 214, Albany, NY, USA

[z] christophe.cardinaud@cnrs-imn.fr

[z] remi.dussart@univ-orleans.fr

Abstract

A silicon oxyfluoride layer was deposited on a-Si samples using SiF_4 / O_2 plasma at different temperatures between -100°C and -40°C. In situ X-Ray Photoelectron Spectroscopy measurements were then performed in order to characterize the deposited layer. The sample was then brought back to room temperature and analyzed again. It has been shown that a temperature below -65°C is needed in order to significantly enhance the physisorption of SiF_x species. Hence, in this condition, a F-rich oxyfluoride layer, stable at low temperature only, is physisorbed. Above this threshold temperature, the native silicon oxide layer is fluorinated and the proportion of O in the deposited layer is higher and remains stable even when the sample is brought back to room temperature.

Introduction

The formation of a silicon oxyfluoride layer has been widely studied for several applications. First, due to its low dielectric constant, the SiO_xF_y layer can be used as an interlayer dielectric in Back-End-Of Line applications and Very-Large-Scale Integration devices [1–3]. Its low refractive index makes it also interesting as optical layer [3–5]. It is also used in plasma structuring [6–11]. This layer is also well-known as the passivation layer used to perform anisotropic deep etch of Si in cryogenic standard and STiGer processes [12–31]. As far as we know, the behavior of the SiO_xF_y layer at cryogenic temperatures has only been investigated for passivation purpose in etching processes, so the knowledge on this layer was based on these studies. It was shown that the SiO_xF_y passivation layer is either built from the SiF_x sites remaining at the silicon surface or by the SiF_x radicals species produced in the plasma from the dissociation of SiF_4 etch by-products. These SiF_x species react with oxygen radicals produced in the plasma to form the SiO_xF_y layer on the cold silicon surface. This layer grows efficiently at low temperature only, and is modified when the sample is brought back to room temperature [30]. Moreover, when the sample is in contact with air, the fluorine content of the SiO_xF_y decreases further and leads to a SiO_x like layer [9,32].
In [29], in situ X-Ray Photoelectron Spectroscopy (XPS) analyses on Si samples after exposure

to SF_6 / O_2 plasma at -100°C were reported. The authors assumed that the deposited SiO_xF_y layer was mainly composed of $SiOF_3$ molecules at the top surface. During the warming of the sample, oxygen and fluorine diffuse more easily at the layer surface. SiF_4 molecules are then formed, and being very volatile, desorb immediately from the surface leading to the layer thickness decrease.
In [32], SiF_4 / O_2 plasma mixture has been produced and studied to evidence the importance of SiF_x physisorption in the formation of the SiO_xF_y layer. It was also shown by Spectroscopic Ellipsometry (SE) measurements that, for the same plasma parameters, the thickness of the deposited layer increases when the sample temperature decreases. Once this layer is brought back to room temperature, a part of it desorbs. The refractive index of the latter layer is close to the one of SiO_2 (1.45) when the deposition is performed above -50°C. However, for a deposition temperature below -50°C, the refractive index decreases down to 1.2 after venting, due to the desorption of physisorbed species, making the layer more porous.
In order to have a better understanding of the mechanisms involved in the growth of the SiO_xF_y layer and its desorption, quasi in situ XPS measurements have been performed and are presented in this paper. The silicon oxyfluoride layer was deposited at three different temperatures between -100°C and -40°C using SiF_4 / O_2 plasma. The layer was analyzed without venting, a first time at the deposition temperature and a second time after warming up the sample.

Experimental

The experiments were conducted on the OPTIMIST platform (Opening of a Technical Platform for the Investigation of the Mechanisms of Interaction between plasma and Surface on a large Temperature range) composed of a home-made ICP reactor connected to a X-ray Photoelectron Spectroscope (XPS). A sketch of this platform is presented in [33]. Tests were performed on a 50 nm thick a-Si layer deposited by Chemical Vapor Deposition (CVD) on a 100 nm thick SiO_2 layer, previously grown on Si substrates. Thus, the SiO_xF_y layer was deposited in the ICP reactor on a 10 x 10 mm^2 a Si coupon. Then, the a-Si coupon was loaded on a transfer sample rod whose temperature is adjustable using liquid nitrogen in combination with a heating resistance. The sample rod can navigate from the reactor chamber to the XPS chamber while keeping the sample under vacuum and at the desired temperature. Leakage tests were carried out before the experiments in order to ensure the absence of leaks and contaminations, and a plasma clean was performed after each experiment. XPS analysis is carried out with an Al Kα monochromatised x-ray source (SPECS XR 50M and Focus 500) operated at 400 W. The analyser (SPECS Phoibos 150HR) operates in fixed transmission and medium area mode. Survey scans are acquired at 30 eV pass energy (PE) with 0.5 eV steps, and high resolution narrow scans at 14 eV PE with 0.05 eV steps. No charge neutraliser was used during data acquisition. Post-acquisition charge correction was found necessary for the -100°C sample only. Considering the overall composition of the layer, this was carried out by aligning the F 1s principal component with that of the F-Si identified for the -65°C sample; the concomitant observation of CF_2 species now at 291.2 eV brought a high confidence in the procedure. We used the software CasaXPS for the quantification and spectral analysis [34].
The a-Si sample was exposed to a 30 s long SiF_4 / O_2 plasma with 6.6 sccm SiF_4 and 20 sccm O_2 flow rates (25 % of SiF_4 in the mixture). The pressure was set to 3.0 Pa and the ICP power

was 200 W.

Results and Discussion

Figure 1. shows the XPS survey spectra of the a-Si surface before and after exposure to SiF_4 / O_2 plasma at -40°C, -65°C and -100°C. Figure 1. a) shows the reference wide scan before SiF_4 / O_2 exposure. Contribution of the Si 2s and Si 2p core levels is observed. Presence of oxygen (O 1s) is due to the native oxide on Si, presence of carbon (C 1s) comes from atmospheric contamination.

According to Figure 1. b) and c), the survey scans obtained after deposition at -40°C and -65°C are quite similar. The main change in comparison to the reference sample is the fluorine contribution (F 1s) and the disappearance of carbon. At -100°C, the fluorine peak becomes very intense, whereas the intensity of the silicon and oxygen peaks decreases sharply. Some physisorbed nitrogen (N 1s) is also detected. It may come from some residual N_2 in the chamber dissociating during the plasma and that physisorb on the cold surface.

For a more accurate analysis, a narrow scan of each core level was performed. As the scans at -40°C and -65°C are quite similar, only -40°C narrow scans will be presented.

Figure 2. shows the narrow scans of the F 1s, O 1s and Si 2p core levels after deposition at -40°C and after warm up. Figure 2. (a) shows F 1s core level. One peak is observed at 687.2 eV, corresponding to F-Si(O) bonds [9,35].

Regarding the O 1s core level in Figure 2. (b), a peak is detected at 533.0 eV. Its slight shift, as compared to the reference sample (532.7 eV) indicates the presence of some O-SiF bonds from the deposited layer in addition to the O-Si from the native oxide.

Figure 2. (c) shows the Si 2p spectra. Two main structures are observed: at 99.2 eV and 103.9 eV, corresponding respectively to the a-Si material and Si_4^+ oxidation state. On the raw sample, the latter is detected at 103.4 eV and comes from the native oxide layer. The shift observed here shows that part of the native oxide has been fluorinated. It also confirms the existence of SiO_xF_y species from the deposited silicon oxyfluoride layer due to the presence of fluorine in the layer [9,16,22,29,35,36]. After warming up, the peaks remain unchanged.

The thickness of the deposited layer after warming up the sample to 20°C was estimated using two different means of calculation. First the QUASES-Tougaard software [37] was used to analyse the evolution of the inelastic background of the Si2s-Si2p spectral region from the reference and the plasma treated samples. Second, the attenuation of the Si 2p (a-Si) component resulting from the presence of the deposited layer was used. Photoelectron attenuation length in the deposited layer was considered similar to that in amorphous SiO_2 and taken as 37.5 Å for Si 2p photoelectrons [38]. Both means of estimation give converging values of 7 ± 3 Å for the SiOF deposited layer. Confidence in this estimation can be evaluated from the calculation of a 17 ± 1 Å thick native oxide on a-Si using the same procedures.

Figure 3. presents the narrow scans of each core levels after deposition at -100°C and after warm up. The F 1s scan in Figure 3. (a) after deposition shows two peaks. The first one is very intense and is detected at 685.5 eV. It is related to F-Si bonds [39] and its intensity strongly decreases after warming up. The second peak is located at 688.5 eV corresponds to F-C bonds [39] due to the physisorption of CF_x species etched from the reactor wall. In agreement, the C 1s spectrum (not shown) presents evidence for CF_x (x = 1 to 3) species. Two others peaks are also

observed after warm up. The first peak at 687.2 eV corresponds to F-SiO bonds, as at -40°C. The second peak at 683.9 eV are identified as F-Cr bonds, such contamination comes from the physisorption of CrF_2 species due to the etching of the Ni/NiCr thermocouple measuring the sample temperature. In fact the sample at low temperature also shows some Cr contamination, but the signal is much weaker; as the latter increases upon warm-up we emphasize that the (nonvolatile) CrF_x species that were dispersed within the SiOF layer are now concentrated at the surface.

Figure 3 (c) presents the Si 2p spectra. After deposition, only the peak at 103.6 eV is detected. The contribution from the a-Si material (99.2 eV) is not observed. This indicates that the sample surface has been totally covered with a SiO_xF_y layer thicker than 10 nm (typical XPS analysis depth assuming an attenuation length of ~3 nm for Si 2p photoelectrons). At this temperature, the desorption rate of physisorbed SiF_x species is lower than at higher temperatures, which leads to an accumulation of SiF_x species at the surface [40]. After warm up, the substrate contribution can be detected again due to the desorption of fluorinated species.

Figure 3 (b) shows the O 1s spectra. The low temperature SiO_xF_y layer gives a contribution at 534.1 eV. Two other oxygen peaks are detected at 541.2 eV and 545.2 eV. They could not be clearly identified. Nevertheless, they may come from some residual species trapped in the physisorbed layer. A similar double contribution is observed on the N 1s region (not shown). After warming up, these species disappear and only one peak, located at 533.0 eV is detected. It is the same as at -40°C and corresponds to O-SiF bonds from the SiO_xF_y layer.

Such evolution shows that the modification of the surface after the deposition at -100°C and after warm up is due to the desorption of SiF_x species. Moreover, this desorption indicates that the deposited layer at -100°C is a mix of a physisorbed layer, only stable at low temperature, and a chemisorbed layer that remains even at room temperature.

Figure 4. shows F 1s and O 1s spectra after deposition at the three different temperatures. It allows to evidence the intermediate behavior at -65°C. Indeed, in Figure 4. (a) a small tail is already detected at 685.5 eV related to F-Si bonds. The intensity of this peak strongly increases when the deposition is performed at -100°C. Moreover, Figure 4. (b) shows that the intensity of O-SiF peak at 533.0 eV slightly drops from about 24000 cps at -40°C to about 20300 cps at -65°C. Moreover, at -100°C, that at 534.1 eV is only about 6100 cps.

Using the acquired scans, the relative surface composition has been quantified after deposition and after heating the sample back to 20°C. The obtained results are presented below in Figure 5.

The experiments performed at -40°C and -65°C lead to very similar results that do not significantly change after heating. The composition averaged on the analyzed depth is about 59% of Si, 23% of O and 17% of F.

At -100°C, it was shown in Figure 3. (c) that the surface is totally covered by a SiO_xF_y layer. According to Figure 5., this layer, including the C, O, N trapped species is composed of 11% of Si, 18% of O, 52 % of F, 4% of C and 15% of N. Skipping the trapped physisorbed species, one obtains 74% F, 8% O and 18% Si. After heating, a significant part of this layer desorbs, which is in agreement with the SE observations reported in [23,29,32]. The F content decreases to 19.5%, which is close to the amount detected at the surface at -40°C and -65°C.

These XPS measurements have first evidenced the existence of a temperature threshold. Indeed, at -65°C and above, the native oxide is fluorinated and a layer with a low amount of

fluorine can be deposited. This SiO_xF_y layer is stable in temperature, as it does not change after bringing the sample back to 20°C. According to [17,32], the material of this layer is close to SiO_2. Being rich in oxygen, it is consequently more resistant to SF_6 plasma.

Below -65°C and more specifically at a temperature close to -100°C, the surface residence time of SiF_x species is significantly increased [40]. The deposited silicon oxyfluoride layer is consequently a mix of chemisorbed molecules and physisorbed fluorine-based species. The physisorbed part of this SiO_xF_y layer is only stable at low temperature, as a significant part of SiF_x is converted in SiF_4 molecules which immediately desorb from the surface once formed during the sample warming up [23]. The thickness decrease observed in [32] is hence due to the depletion of SiF_x species from the surface layer.

Conclusions

This study presents the effect of temperature on the deposition of a SiO_xF_y layer on a-Si. It shows that the concentration of fluorine atoms in the deposited SiO_xF_y layer increases when decreasing the temperature below -65°C. Then, a decrease in the Si-O peak intensity and the formation of a small peak related to Si-F bonds can be clearly observed by in situ XPS analysis. At -100°C, the SiO_xF_y layer has a stoichiometric composition close to a $SiOF_3$ as reported in [29] with a SF_6 / O_2 plasma in overpassivating regime. This study also confirms that the layer is significantly modified during the warming of the sample with a large depletion of SiF_x species from the layer. Thus, once warmed up, there is no significant difference in the composition of the deposited SiO_xF_y layer regarding the deposition temperature. However, in a previous study [32] although performed under different conditions, the authors showed that when depositing a SiO_xF_y layer at low temperature (close to -100°C) and then warming it up, the created layer is porous. This is due to the desorption of SiF_x species, and the layer will consequently have a different optical index than if it was deposited at room temperature.
Finally, this study showed that at -40°C and -65°C, a chemisorbed SiO_xF_y layer can be formed by first fluorinating the native oxide, whereas at -100°C, the physisorption of SiF_x species is enhanced and thus the deposited layer is a mix of chemisorbed and physisorbed species.

Thus, this study offers further insights into the mechanisms involved in processes using SiF_4 / O_2 plasma, which is used in the so-called STiGer cryogenic etching processes [41]. However, it also offers the possibility to tune the SiO_xF_y chemical and optical layer properties as desired, by adjusting the temperature of deposition.

Acknowledgments

The authors gratefully thank Shigeru Tahara from TEL for all the helpful discussions and also Kumiko Yamazaki and Nagisa Sato from TEL for their support to the project.
This work was supported by CERTeM 5.0 platform, which provides most of the equipment; the CNRS-Réseau des Plasmas Froids is also acknowledged for giving access to the Optimist platform. This work was partially financed by the French ‘Agence Nationale de la Recherche’ through Contract No ANR-20-CE24-0014-02 under the name PSICRYO project.

References

1. J. H. Burkhart, D. Denison, J. C. Barbour, and C. A. Apblett, *Nucl. Instr. and Meth. in Phys. Res. B,* **118**, 698–703 (1996).

2. H. Geisler, in *AIP Conference Proceedings*,, vol. 817, p. 277–287, AIP, Dresden (Germany) (2006) http://aip.scitation.org/doi/abs/10.1063/1.2173560.

3. J. H. Lee and C. K. Hwangbo, *Surface and Coatings Technology*, **128–129**, 280–285 (2000).

4. S.-H. Jeong, J. Nishii, H.-R. Park, J.-K. Kim, and B.-T. Lee, *Surface and Coatings Technology*, **168**, 51–56 (2003).

5. J. Zhang and E. R. Fisher, *J. Appl. Phys*, **96**, 1094–1103 (2004).

6. C. Yang, S.-H. Ryu, Y.-D. Lim, and W. J. Yoo, *Nano*, **03**, 169–173 (2008).

7. M. Gaudig et al., *32nd European Photovoltaic Solar Energy Conference and Exhibition*, 4 (2016).

8. J. Gao, M. de Raad, B. P. Bowen, R. N. Zuckermann, and T. R. Northen, *Anal. Chem.*, **88**, 1625–1630 (2016).

9. M. Gaudig et al., *J. Appl. Phys*, **121**, 063301 (2017).

10. X. Huang, S. Gluchko, R. Anufriev, S. Volz, and M. Nomura, *ACS Appl. Mater. Interfaces*, **11**, 34394–34398 (2019).

11. M. H. Richter, M. Lublow, K. M. Papadantonakis, N. S. Lewis, and H.-J. Lewerenz, *ACS Appl. Mater. Interfaces*, **12**, 17018–17028 (2020).

12. S. Tachi, K. Tsujimoto, and S. Okudaira, *Appl. Phys. Lett.*, **52**, 616–618 (1988).

13. S. Tachi, K. Tsujimoto, S. Arai, and T. Kure, *J. Vac. Sci. Technol. A*, **9**, 796–803 (1991).

14. K. Tsujimoto, S. Okudaira, and S. Tachi, *Jpn. J. Appl. Phys.*, **30**, 3319–3326 (1991).

15. J. W. Bartha, J. Greschner, M. Puech, and P. Maquin, *Microelectron. Eng.*, **27**, 453–456 (1995).

16. G. S. Oehrlein, K. K. Chan, M. A. Jaso, and G. W. Rubloff, *J. Vac. Sci. Technol. A*, **7**, 1030–1034 (1989).

17. G. S. Oehrlein and Y. Kurogi, *Mater. Sci. Eng., R*, **24**, 153–183 (1998).

18. S. Aachboun and P. Ranson, *J. Vac. Sci. Technol. A*, **17**, 2270–2273 (1999).

19. S. Aachboun, P. Ranson, C. Hilbert, and M. Boufnichel, *J. Vac. Sci. Technol. A*, **18**, 1848–1852 (2000).

20. M. Boufnichel, S. Aachboun, F. Grangeon, P. Lefaucheux, and P. Ranson, *J. Vac. Sci. Technol. B*, **20**, 1508 (2002).

21. M. Boufnichel, S. Aachboun, P. Lefaucheux, and P. Ranson, *J. Vac. Sci. Technol. B*, **21**, 267

(2003).

22. R. Dussart et al., *J. Micromech. Microeng.*, **14**, 190 (2003).

23. X. Mellhaoui et al., *J. Appl. Phys*, **98**, 104901 (2005).

24. M. Boufnichel, P. Lefaucheux, S. Aachboun, R. Dussart, and P. Ranson, *Microelectron. Eng.*, **77**, 327–336 (2005).

25. R. Dussart et al., *J. Phys. D: Appl. Phys.*, **38**, 3395–3402 (2005).

26. T. Tillocher et al., *J. Vac. Sci. Technol. A*, **24**, 1073–1082 (2006).

27. R. Dussart et al., *Microelectron. Eng.*, **84**, 1128–1131 (2007).

28. A. F. Isakovic, K. Evans-Lutterodt, D. Elliott, A. Stein, and J. B. Warren, *J. Vac. Sci. Technol. A*, **26**, 1182–1187 (2008).

29. J. Pereira et al., *Appl. Phys. Lett.*, **94**, 071501 (2009).

30. M. A. Blauw, T. Zijlstra, R. A. Bakker, and E. Van der Drift, *J. Vac. Sci. Technol. B*, **18**, 3453 (2000).

31. H. V. Jansen et al., *J. Micromech. Microeng.*, **20**, 075027 (2010).

32. G. Antoun et al., *Jpn. J. Appl. Phys.*, **58**, SEEB03 (2019).

33. https://www.cnrs-imn.fr/index.php/themes/procedes-de-gravure/593-reacteur-plasma-optimist-2.

34. http://www.casaxps.com/.

35. Ch. Cardinaud and G. Turban, *Applied Surface Science*, **45**, 109–120 (1990).

36. S. Tajima, T. Hayashi, K. Ishikawa, M. Sekine, and M. Hori, *J. Phys. Chem. C*, **117**, 20810–20818 (2013).

37. http://www.quases.com/products/quases-tougaard/.

38. S. Tanuma, C. J. Powell, and D. R. Penn, *Surf. Interface Anal.*, **21**, 165–176 (1994).

39. C. Cardinaud, A. Rhounna, G. Turban, and B. Grolleau, *J. Electrochem. Soc.*, **135**, 1472 (1988).

40. S. Tinck, E. C. Neyts, and A. Bogaerts, *J. Phys. Chem. C*, **118**, 30315–30324 (2014).

41. T. Tillocher et al., *J. Electrochem. Soc.*, **155**, D187 (2008).

Figures

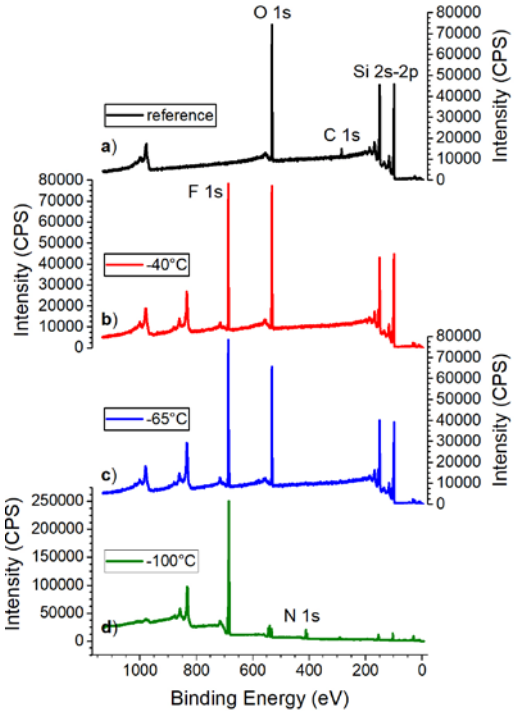

Figure 1. XPS survey scans on a-Si coupon before and after SiF_4 / O_2 plasma exposure at three different temperatures (Experimental conditions: SiF_4 / O_2 plasma: 25%, 30 s, 3 Pa, 200 W)

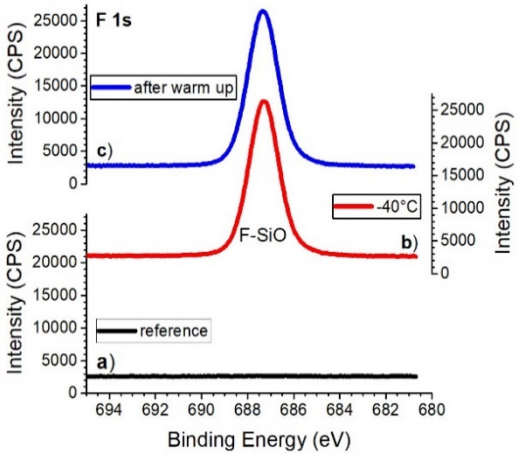

(a)

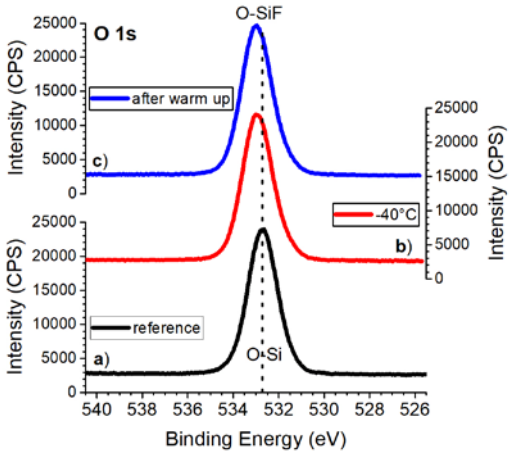

(b)

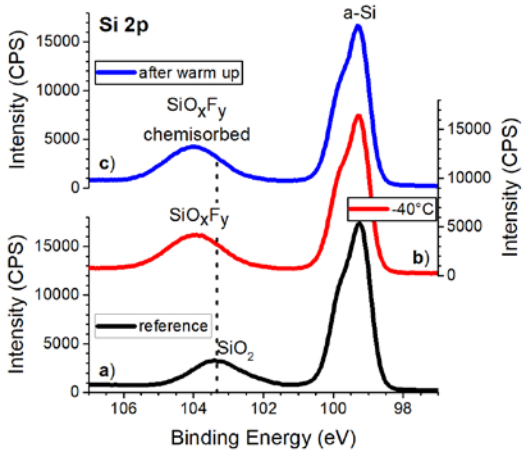

(c)

Figure 2. XPS scans on a-Si coupon after SiF_4 / O_2 plasma exposure at -40°C and after warming up (a) F 1s, (b) O 1s, (c) Si 2p (Experimental conditions: SiF_4 / O_2 plasma: 25%, 30 s, 3 Pa, 200 W)

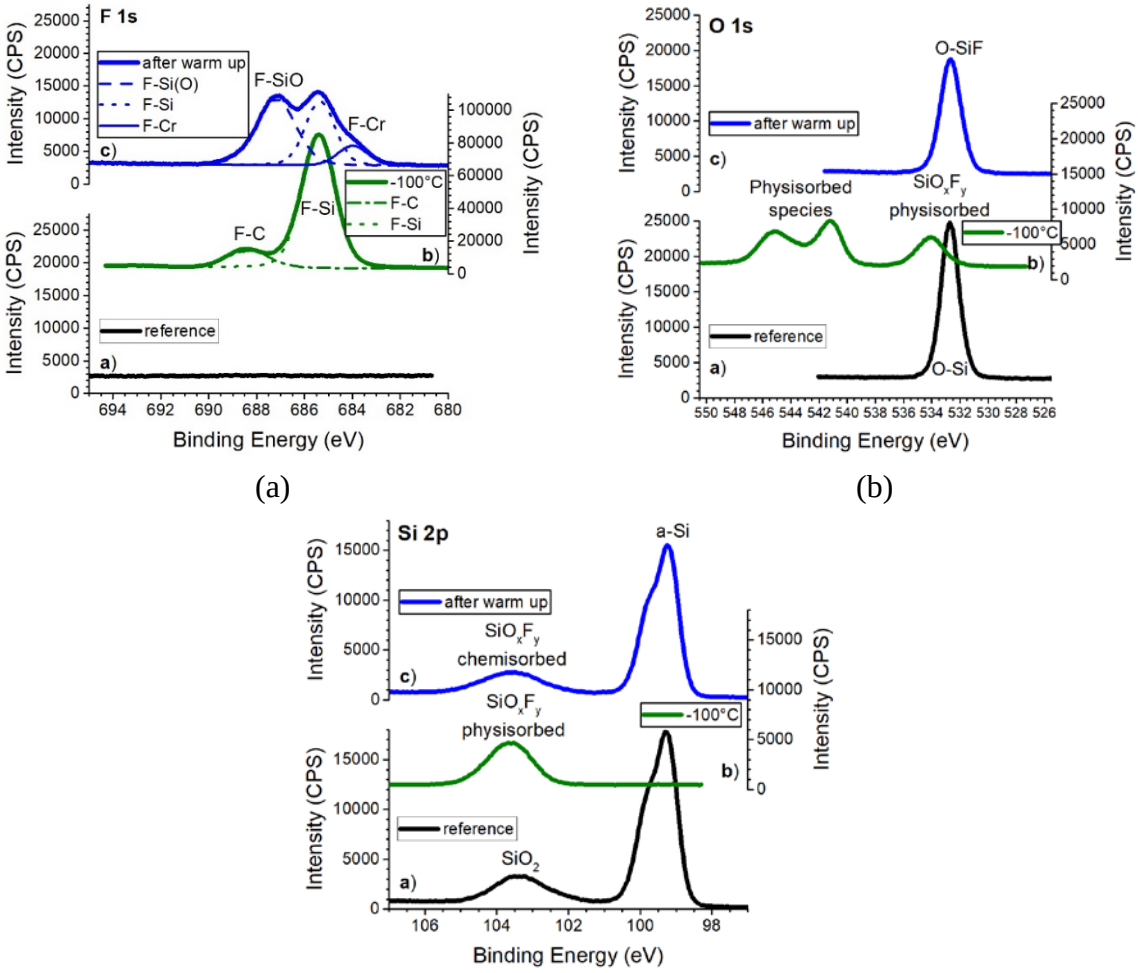

(a) (b)

(c)

Figure 3. XPS scans on a-Si coupon after SiF_4 / O_2 plasma exposure at -100°C and after warming up (a) F 1s, (b) O 1s, (c) Si 2p (Experimental conditions: SiF_4 / O_2 plasma: 25%, 30 s, 3 Pa, 200 W)

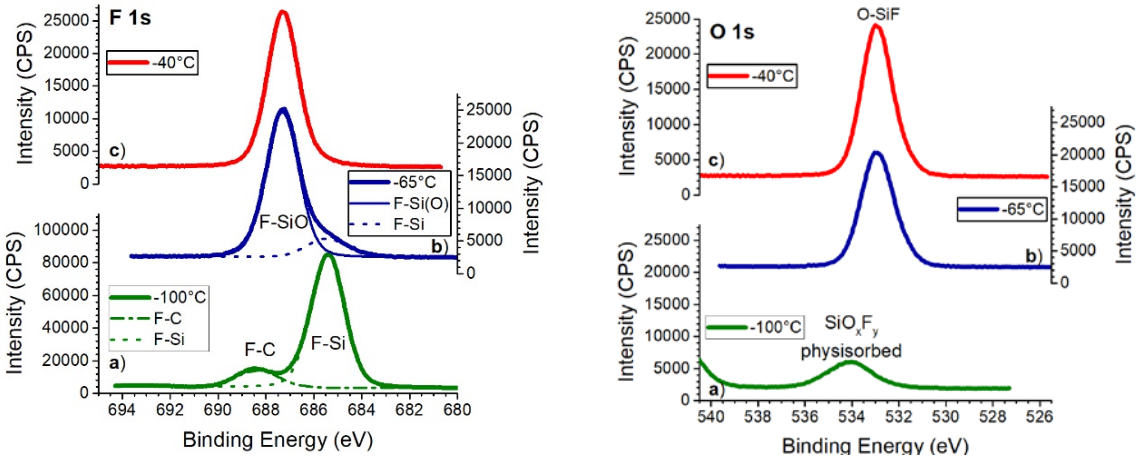

(a) (b)

Figure 4. XPS scan on a-Si coupon after SiF_4 / O_2 plasma exposure at -40°C, -65°C and -100°C (a) F 1s, (b) O 1s

(Experimental conditions: SiF_4 / O_2 plasma: 25%, 30 s, 3 Pa, 200 W)

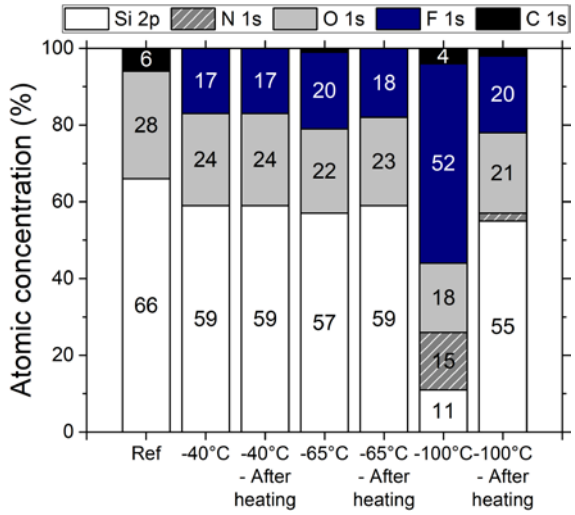

Figure 5. Quantification of surface composition after SiF_4 / O_2 plasma and after warming back the sample to 20°C. Uncertainty is ± 2%.

(Experimental conditions: SiF_4 / O_2 plasma: 25%, 30 s, 3 Pa, 200 W)